JOURNAL OF GEOPHYSICAL RESEARCH, VOL. 106, NO. C2, PAGES 2761-2778, FEBRUARY 15, 2001

Flow of bottom water in the northwestern Weddell Sea

Eberhard Fahrbach, Sabine Harms[1], Gerd Rohardt, Michael Schröder and Rebecca A. Woodgate[2]

Alfred Wegener Institute for Polar and Marine Research, Bremerhaven, Germany

Abstract. The Weddell Sea is known to feed recently formed deep and bottom water into the Antarctic circumpolar water belt, from whence it spreads into the basins of the world ocean. The rates are still a matter of debate. To quantify the flow of bottom water in the northwestern Weddell Sea data obtained during five cruises with R/V *Polarstern* between October 1989 and May 1998 were used. During the cruises in the Weddell Sea, five hydrographic surveys were carried out to measure water mass properties, and moored instruments were deployed over a time period of 8.5 years to obtain quasi-continuous time series. The average flow in the bottom water plume in the northwestern Weddell Sea deduced from the combined conductivity-temperature-depth and moored observations is 1.3±0.4 Sv. Intensive fluctuations of a wide range of timescales including annual and interannual variations are superimposed. The variations are partly induced by fluctuations in the formation rates and partly by current velocity fluctuations related to the large-scale circulation. Taking into account entrainment of modified Warm Deep Water and Weddell Sea Deep Water during the descent of the plume along the slope, between 0.5 Sv and 1.3 Sv of surface-ventilated water is supplied to the deep sea. This is significantly less than the widely accepted ventilation rates of the deep sea. If there are no other significant sources of newly ventilated water in the Weddell Sea, either the dominant role of Weddell Sea Bottom Water in the Southern Ocean or the global ventilation rates have to be reconsidered.

1. Introduction

In the deep basins of the global ocean, water colder than 2°C is commonly called Antarctic Bottom Water. It originates from water masses which were recently formed in the Southern Ocean, from which they spread into the Atlantic, Indian, and Pacific Oceans [*Reid and Lynn*, 1971; *Mantyla and Reid*, 1983]. In the Southern Ocean, water mass formation occurs in the subpolar gyres and at their rims through atmosphere-ice-ocean interaction [*Carmack*, 1986; *Baines and Condie*, 1998] as well as through mixing with adjacent water masses. The most prominent area of water mass formation in the Southern Ocean is the Weddell Sea [*Brennecke*, 1921; *Deacon*, 1933; *Wüst*, 1933; *Mosby*, 1934; *Carmack*, 1977; *Rintoul*, 1998].

While the regional distribution of the water masses of different origins is well studied [*Carmack*, 1977; *Rintoul*, 1998], there is still a large uncertainty about their rates of formation. Recent estimates of the Southern Ocean's contribution to ventilate the deep ocean range between 10 and 15 Sv [*Broecker et al.*, 1998, 1999; *Orsi et al.*, 1999; also S. Peacock et al., submitted manuscript, 2000]. Large-scale water mass distributions suggest the southern contribution to be comparable to the formation rate of North Atlantic Deep Water [*Broecker et al.*, 1998]. Deep water formation in the Weddell Sea occurs to a large extent through bottom water formation. Weddell Sea Bottom Water, mostly confined to the Weddell basin [*Orsi et al.*, 1993], mixes with adjacent water masses derived from Circumpolar Deep Water to form Weddell Sea Deep Water, which then spreads into the global ocean. As a consequence, the properties of Weddell Sea Deep Water are to a large extent controlled by the formation of Weddell Sea Bottom Water. However, there is also evidence that part of the Weddell Sea Deep Water is formed directly by plumes descending from the shelf [*Orsi et al.*, 1993; *Fahrbach et al.*, 1995; *Orsi et al.*, 1999; *Meredith et al.*, 2000]. The aim of this study is to quantify the outflow of Weddell Sea Bottom Water in the western Weddell Sea, from which the contribution of the Weddell Sea to the formation rate of deep water masses may be deduced.

The water mass properties on a transect across the southern Weddell Sea between Joinville Island and Kapp Norvegia reflect the gyre circulation, with southwestward flow in the east and northeastward flow in the west (Figures 1 and 2). The upper layer waters consist of Winter Water, Antarctic Surface Water, and shelf waters, collectively referred to as surface water, with temperatures less than 0°C. The deepening of the surface layer toward the coast due to an on-shore Ekman transport and convection in the coastal polynya is clearly visible on both sides of the section. At greater depths the inflow of relatively warm and saline Warm Deep Water into the southern Weddell Sea occurs in the eastern part of the transect [*Carmack and Foster*, 1975; *Foster and Carmack*, 1976a, 1976b; *Orsi et al.*, 1993]. The outflow in the west in the level of the Warm Deep Water is noticeably colder and less saline than the inflow in the east. The cold water mass below the Warm Deep Water consists of Weddell Sea Deep Water [*Reid et al.*, 1977; *Orsi et al.*, 1993]. On the western slope a layer of newly formed Weddell Sea

[1] now at: Institut für Meereskunde an der Universität Kiel, Düsternbrooker Weg 20, D-24105 Kiel, Germany

[2] now at: Applied Physics Laboratory, University of Washington, 1013 NE 40th Street, Seattle, Washington 98105-6698, U.S.A.

Paper number 2000JC900142.
0148-0227/01/2000JC900142$09.00

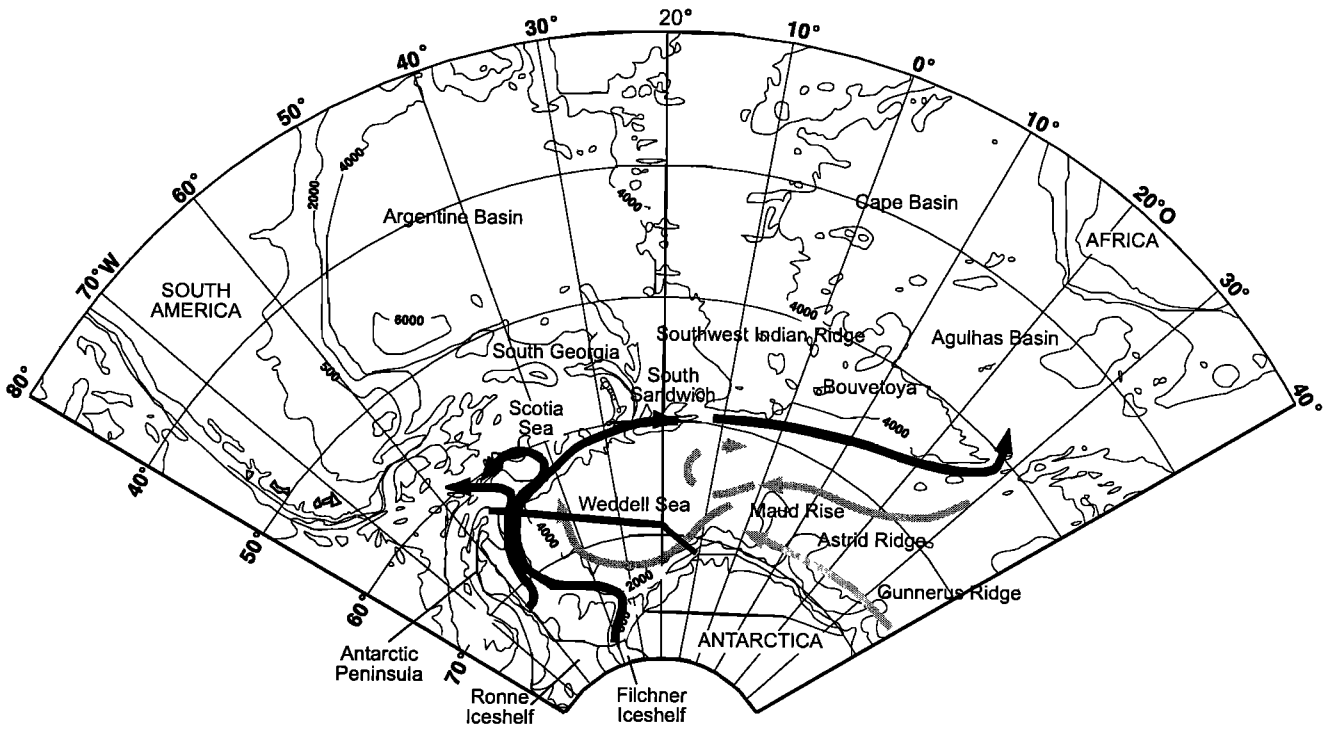

Figure 1. Schematic representation of the circulation in the western Weddell Sea and the location of the transect displayed in Figure 2.

Bottom Water, defined by potential temperatures less than -0.7°C and salinities below 34.65, flows to the north [*Gordon et al.*, 1993; *Fahrbach et al.*, 1994, 1995; *Muench and Gordon*, 1995; *Gordon*, 1998].

The outflow of newly formed bottom water in the western Weddell Sea has been monitored by conductivity-temperature-depth (CTD) transects and moored instruments over a period of more than 8 years between 1989 and 1998. Results based on the first three years of data obtained from a subset of moored observations show that the outflow of Weddell Sea Bottom Water fluctuates significantly on annual and interannual timescales, varying in strength between 1 and 4 Sv [*Fahrbach et al.*, 1995]. The better coverage of the more recent data set in time as well as in space allows us to improve the previous estimates.

2. Data

The present work is based on observations obtained from the R/V *Polarstern* between 1989 and 1998. The sections were part of the World Ocean Circulation Experiment (WOCE) "Repeat Sections" Programme. The locations of the CTD stations from the various cruises are shown in Figure 3. Data from five surveys in the southern Weddell Sea between Kapp Norvegia and Joinville Island are used: survey ANT VIII/2: September 12, 1989, to October 8, 1989; survey ANT IX/2: November 22, 1990, to December 15, 1990; survey ANT X/7: December 18, 1992, to January 12, 1993; survey ANT XIII/4: April 25, 1996, to May 9, 1996; and survey ANT XV/4: April 1, 1998, to April 9, 1998.

Between 1989 and 1994 a Neil Brown Mark III CTD probe was used together with a General Oceanics, Inc., rosette water sampler with twenty-four 12-Litre bottles. Since 1995 a Falmouth Scientific Instruments (FSI) Triton Integrated CTD probe was used in combination with a twenty-four 12-Litre bottle rosette from General Oceanics, Inc., controlled by a water bottle release mechanism from FSI. The accuracy of the data set is based on laboratory calibrations by the Scripps Institution of Oceanography and FSI both before and after the cruise. The precruise calibrations were used on board, and the accuracy of the instruments was further controlled during the cruise by use of reversing digital and mercury thermometers and pressure meters. The conductivity readings of the CTD were corrected by using salinity measurements from the rosette water samples, determined by a Guildline Autosal 8400A salinometer referenced to International Association for Physical Sciences of the Oceans (IAPSO) Standard Sea water. All salinities are quoted according to the UNESCO Practical Salinity Scale (PSS78). The final data are accurate to 3 mK in temperature, 2 dbar in pressure and 0.003 in salinity [e.g., *Bathmann et al.*, 1992, 1994; *Fahrbach and Gerdes*, 1997; *Fahrbach*, 1999].

In the framework of an extensive mooring program, four current meter moorings were maintained on the western part of the transect from Kapp Norvegia to Joinville Island between 1989 and 1998 with some time gaps (Figures 3 and 4 and Table 1) [*Fahrbach et al.* 1994; *Fahrbach*, 1999]. Mostly Aanderaa recording current meters were deployed, along with few acoustic current meters from EG&G and FSI three-dimensional acoustic current meters. The thermistors of the Aanderaa and the FSI instruments were calibrated by the manufacturer before and after the mooring period. Since the accuracy of the CTD sensors is an order of magnitude better than that of the moored instruments, the records of the moored instruments were corrected with a constant offset to match the CTD profiles at the times of deployment and recovery of the instruments. The accuracy of the current meters is achieved through maintenance by the manufacturer. It is given as ±1 cm/s for the Aanderaa and ±0.5

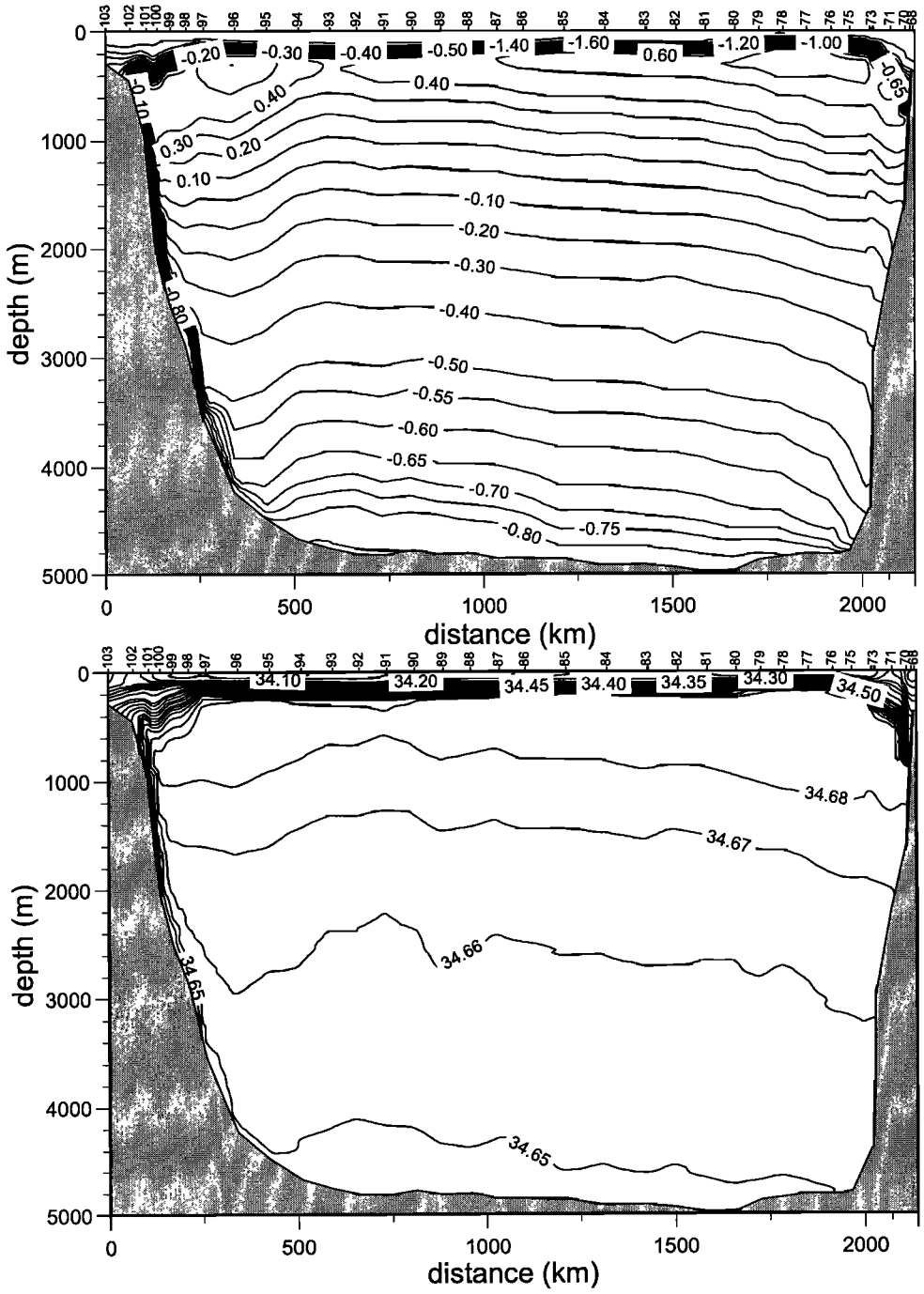

Figure 2. Vertical section of potential temperature (top) and salinity (bottom) across the southern Weddell Sea from Kapp Norvegia (right) to Joinville Island (left) measured from R/V *Polarstern* during ANT XIII/4 from April 25, 1996, to May 9, 1996.

cm/s for the FSI current meters. Currents were sampled every 2 hours and then averaged to yield daily estimates. Threshold problems did not occur since the currents were always stronger than 1.5 cm/s.

Meteorological observations near the mooring sites were available from the analyses of the European Centre for Medium-Range Weather Forecasts (ECMWF). The ECMWF analyses include data from manned and unmanned stations by the ECMWF assimilation procedure (ECMWF, 1992). The spatial resolution of the ECMWF data is 1.125° both for latitude and longitude, and the time resolution is 6 hours.

3. Bottom Water Plume

Weddell Sea Bottom Water is defined by a potential temperature of less than -0.7°C [e.g., *Reid et al.*, 1977; *Orsi et al.*, 1993]. The outflow of bottom water from the formation area in the southwestern Weddell Sea toward the northern limb of the

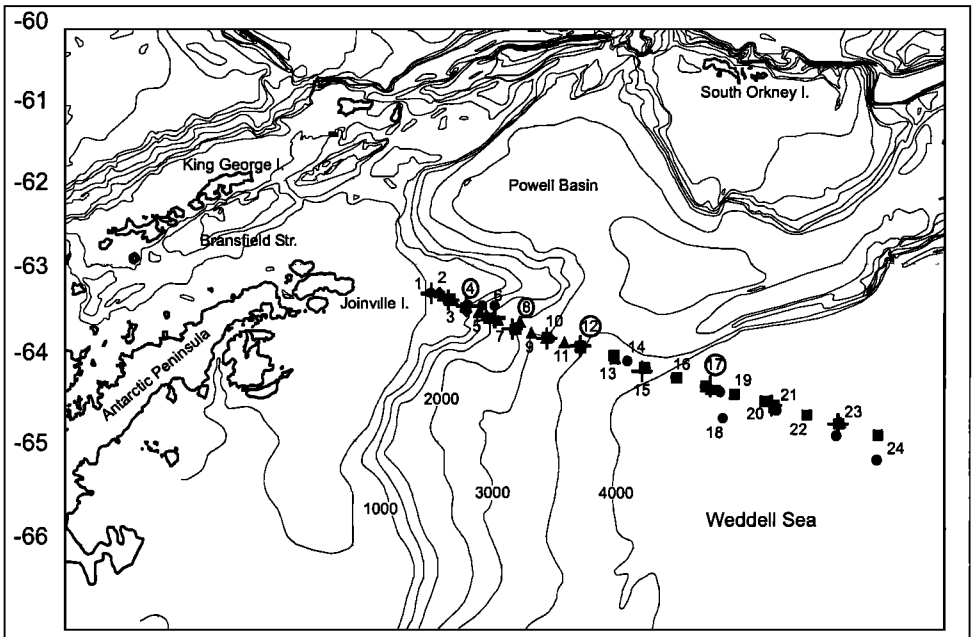

	1	2	3	4	5	6	7	8	9	10	11	12
ANT VIII/2 ●	145		146	147	149	150		151		152		153
ANT IX/2 +	39		41	42		43		44		45		46
ANT X/7 ■			72	69				65		64		63
ANT XIII/4 ◆		102		101		100		99		98		97
ANT XV/4 ▲		4	5		6, 8	10	9	11	12	13	14	15
Mooring				206				207				216

	13	14	15	16	17	18	19	20	21	22	23	24
ANT VIII/2 ●		154		155	156	157			158		159	160
ANT IX/2 +			47		48				49		50	
ANT X/7 ■	62		61	60	59		58	57	56	55	54	53
ANT XIII/4 ◆			96		95				94		93	
ANT XV/4 ▲	16		17		18				19		20	
Mooring					217							

Figure 3. Station map of the five cruises made between 1989 and 1998. The different cruises (ANT VIII/2 to ANT XV/4) are displayed by different symbols. The stations are grouped in reference to 24 repeat locations. The station numbers of each cruise are listed under the nearest repeat location. The moorings are indicated by circles around the nearest repeat location.

Weddell gyre (Figures 1 and 2) was observed at the northern tip of the Antarctic Peninsula on a transect toward the central Weddell Sea. The bottom water plume structure during the five CTD surveys is displayed in terms of transects of potential temperature in a 400-m-thick bottom layer along the seafloor (Figures 4 and 5), as well as in terms of vertical profiles near mooring location 207 in the center of the plume (Figure 6). The transects reached from the shelf break, taken as the location of the 400-m depth contour, into the Weddell basin.

In the bottom layer the temperatures below –0.7°C were found in a plume approximately 250 km wide and 250 m thick, which descended along the northwestern slope of the Weddell Sea between 1250 m and 3000 m (Figure 5). In spite of significant variability the plume was located during all surveys between 40 and 275 km from the shelf break. The cross-section area of the bottom water plume ranged from 37 to 56 km^2 (Table 2). The potential temperature minimum in the plume varied between -1.143° and -1.345°C. The coldest outflow with a minimum temperature of -1.345°C and an average plume temperature of -1.035°C occurred in April 1998 simultaneously with the largest layer thickness. Salinity does not appear to be related to temperature as both the coldest and the warmest plume waters have the same salinity of 34.623, which is in the center of the full range between 34.608 and 34.640. The vertical profiles (Figure 6) displayed a generally well mixed bottom boundary layer, 35 m to 80 m thick, and a quasi-linear transition to the Weddell Sea Deep Water. In some sections the plume was formed by two cold water cores about 50 km apart. At times the two distinct cores were of similar intensity (ANT VIII/2-1989 and ANT XV/4-1998); at other times, one core was significantly stronger than the other, and the weaker core appeared to be merged into the stronger one.

Toward the shelf a frontal system separated the Weddell Sea Bottom Water from the Warm Deep Water and the shelf water. Although the intensity of this front varied from survey to survey, its location was remarkably constant. At times the warm core of the modified Warm Deep Water reached the bottom layer (ANT VIII/2-1989); at other times the cold shelf water layer merged into the bottom water (ANT X/7-1992/93). Toward the gyre center, about 275 to 375 km from the shelf break, the bottom

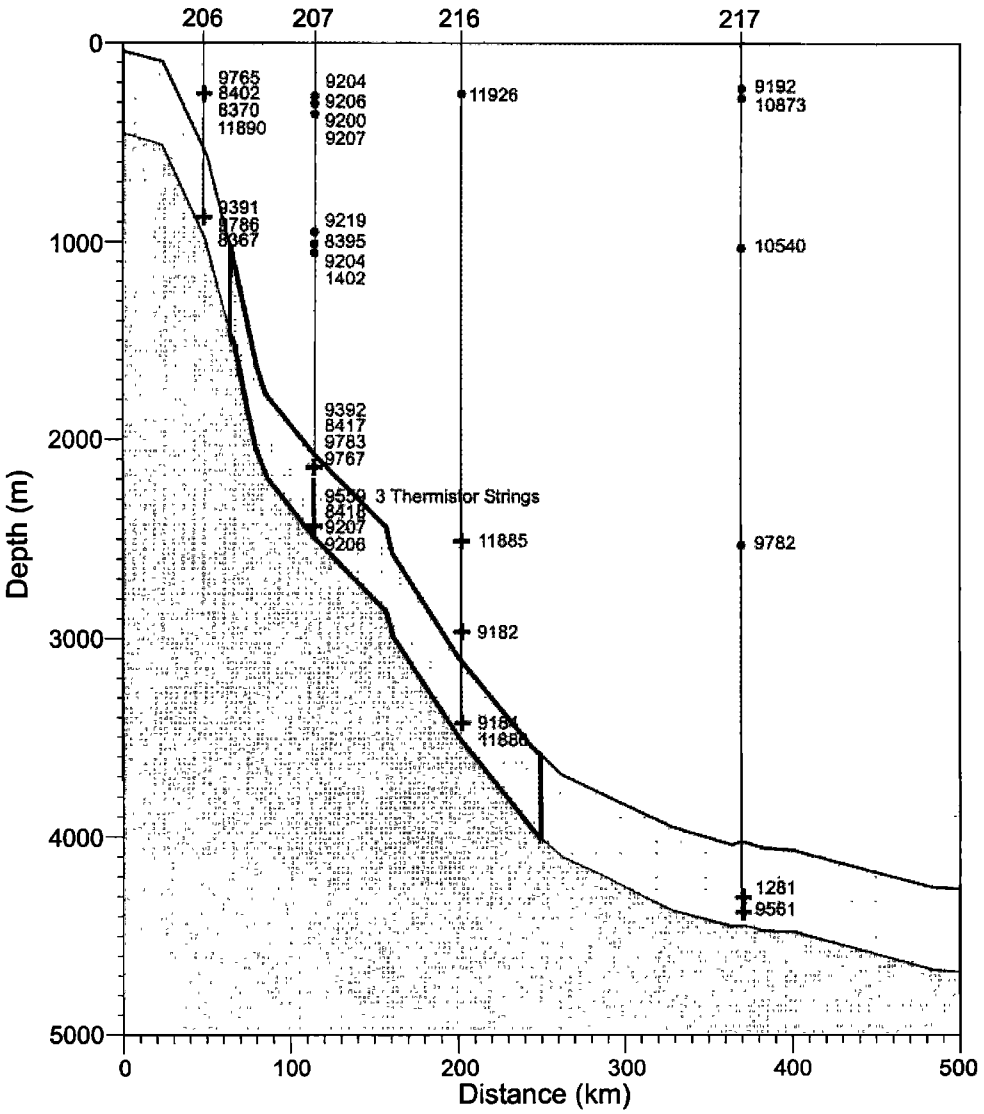

Figure 4. Vertical section along the five cruise tracks as displayed in Figure 3, showing the moored current meters and thermistor strings of four observation periods from 1989 until 1998. At each location the availability of a record is indicated by the instruments' serial numbers marked right of the location. The near-bottom layer displayed in Figure 5 is shaded. The instruments used to calculate the flow in the bottom water plume as displayed in Figure 8 are marked by pluses.

Table 1. Time Series Available During the Four Mooring Periods Which Are Used for the Estimates of the Outflow of Weddell Sea Bottom Water in the Northwestern Weddell Sea

	Period 1	Period 2	Period 3	Period 4
Deployment cruise	ANT VIII/2	ANT IX/2	ANT X/7	ANT XIII/4
Start date	Sept. 20, 1989	Jan. 13, 1991	Jan. 16, 1993	May. 13, 1996
Recovery cruise	ANT IX/2	ANT X/7	ANT XIII/4	ANT XV/4
Stop date	Nov. 17, 1990	Oct. 29, 1992	Feb. 6, 1995	Mar. 28, 1998
Record length, days	424	656	752	685
Gap between mooring periods, days		57	79	461
Moorings deployed	206	206	206	206
during the period	207	207	207	207
		216		216
		217	217	
Number of current meters	6	10	9	8
Thermistor string in mooring AWI207	no	yes	yes	yes

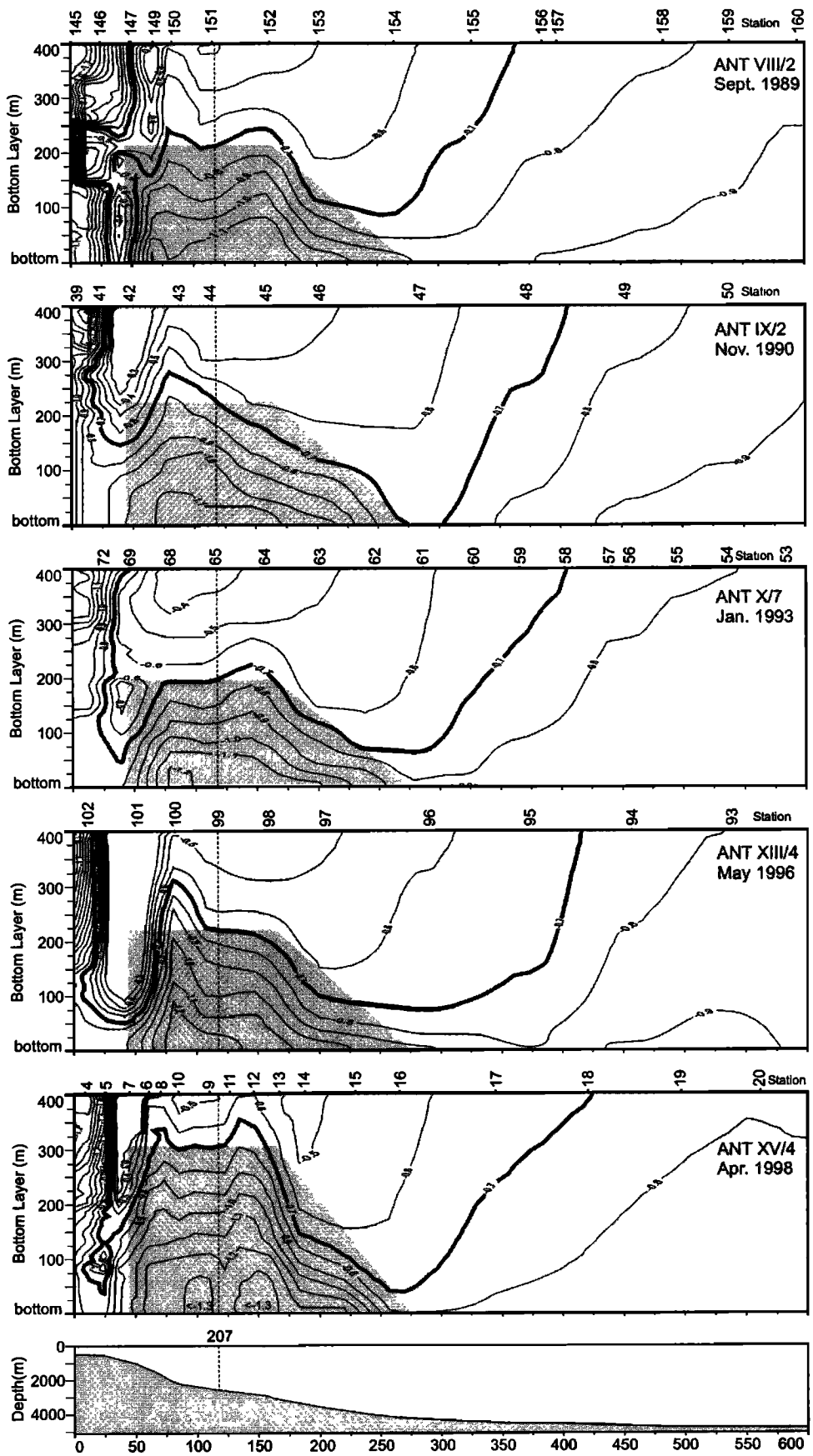

Figure 5a. The potential temperature contour plot of the 400-m-thick bottom layer along the transect as shown in Figure 4 for the five cruises from 1989 until 1998. The bottom plot shows the depth profile along the transect. The –0.7°C isotherm of the potential temperature indicates the upper boundary of the Weddell Sea Bottom Water. The vertical dashed line in each contour plot marks the location of the thermistor string from mooring 207. The shaded area is the best fit of a trapezium determined from the thickness of the bottom water plume at the mooring 207.

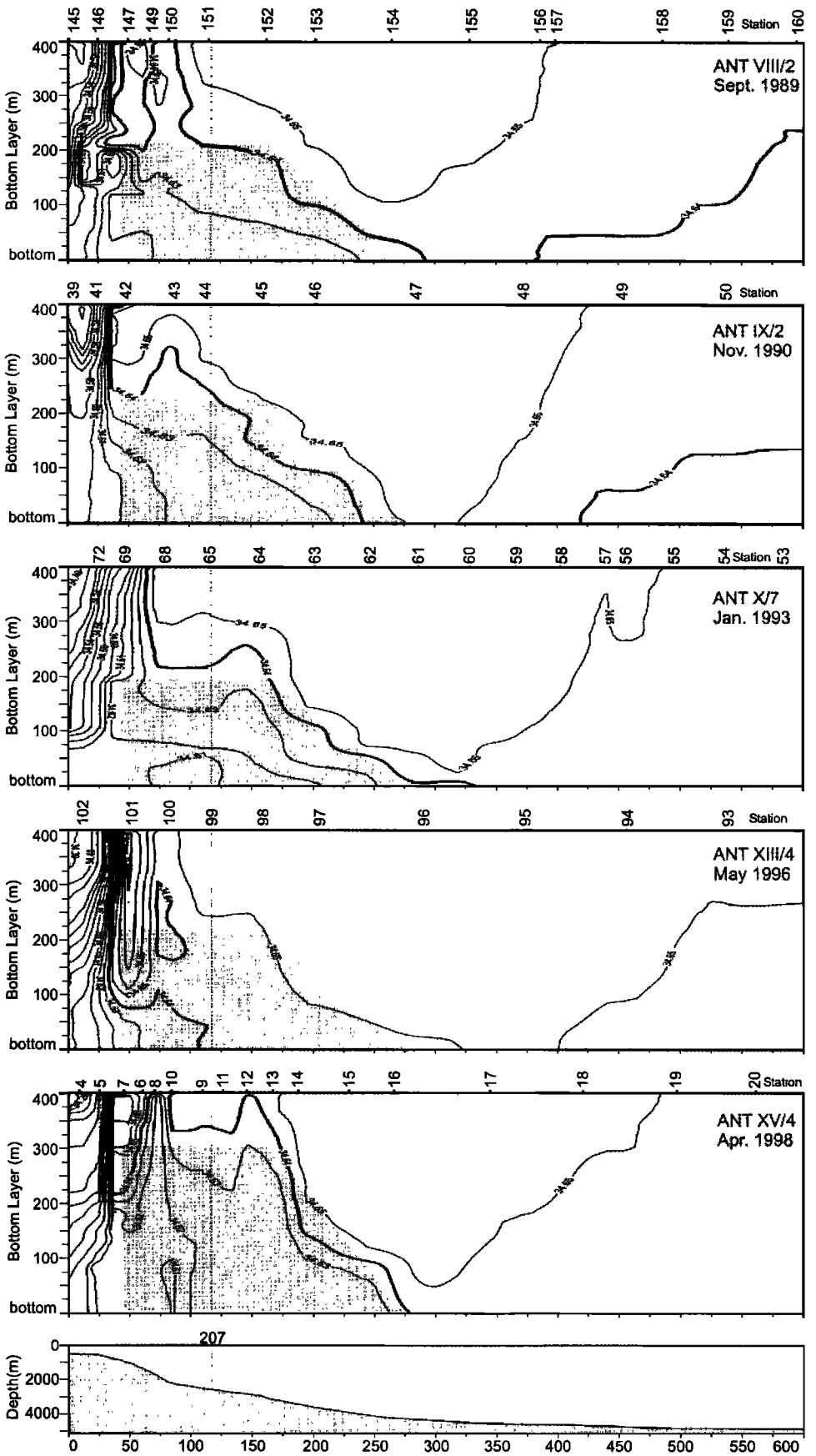

Figure 5b. As in Figure 5a, except for salinity. The 34.64 isoline is highlighted.

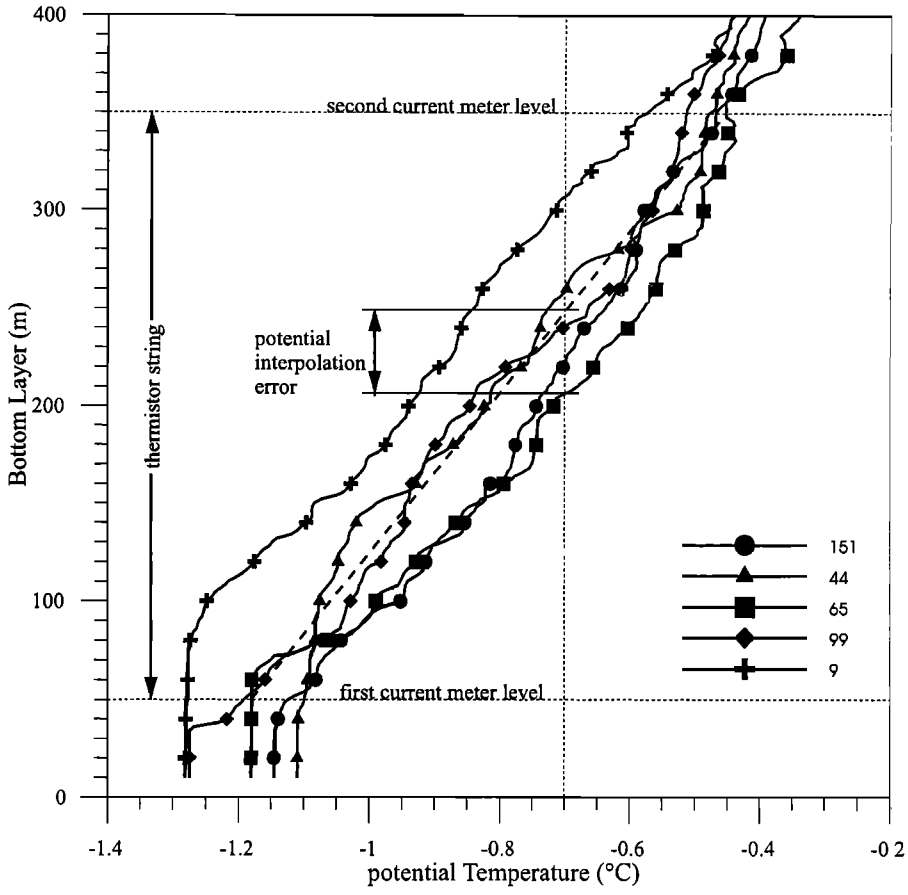

Figure 6. Bottom 400 m of CTD profiles of potential temperature near mooring 207 enlarged for the 400-m-thick bottom layer. The stations are indicated by different symbols. The station number and the year are given in the inset (lower right corner). The depth of the current meters and the temperature boundary of the bottom water plume (-0.7°C) are indicated by dashed lines. Corresponding temperatures from current meter records were available 50 m and 350 m off the bottom to determine the thickness of the bottom layer for the first mooring period from 1989 to 1990. From January 1991 on, thermistor strings were deployed to determine the layer thickness. This reduces the potential interpolation error to less than 10 m.

water layer in the central Weddell Sea was separated from the plume over the continental slope by a temperature maximum. The salinity sections (Figure 5b) show the same features as the potential temperature sections. During to the lack of appropriate time series of salinity from the moored instruments, the water mass boundary was determined in the following analysis by potential temperature only.

For the time periods when CTD data were available, the cross-section area of the plume was obtained with an accuracy of approximately 20 km in the horizontal (depending on the distance to the station) and 2 m in the vertical. At other times, cross-section area of the plume was derived from the measurements of the moored instruments. The horizontal distance of the moorings ranged between 60 km and 170 km. With the exception of mooring 207, where thermistor cables were deployed from 1990 onward, the instruments were separated by several hundred meters in the vertical, thus reducing the accuracy of the cross-section area estimate significantly (Figure 4). To improve the quality of the plume area estimate derived from the moored time series, we took advantage of the stability of the plume shape supported by the five CTD transects (Figure 5).

The two adjacent cores generate a trapezium-shaped plume. It can be approximated by an area with constant baseline about 235 km long, a constant boundary in the northwest 40 km from the shelf break (defined by the front to the modified Warm Deep Water), an upper boundary about 122 km long but variable in height, and a variable boundary in the southeast which depends on the height of the trapezium (shaded area in Figure 5). The length of the upper boundary was determined so that the difference between the original plume area, obtained from the high-resolution CTD observations, and the trapezium-shaped approximation is less than 10% (Table 2). To test the quality of this approximation, the area of the trapezium was compared to the area derived from the CTD data based on the 1 km by 2 m grid. The rms deviation between the gridded and the trapezium-shaped plume area amounts to 2.6% for the five CTD surveys. Since during the first year (from 1989 to 1990) temperature measurements were available only 50 m and 350 m above the bottom (Table 1), the potential error in the depth of the -0.7°C isotherm may reach 40 m due to the deviation of the profiles from a linear shape (Figure 6). From 1990 onward, thermistor cables were deployed at mooring 207. The thermistors measure temperature with a vertical resolution of 25 m, thus reducing the

Table 2. Characteristics of Weddell Sea Bottom Water Plume on the Transect off Joinville Island During the Five Surveys[a].

	Cruise				
	ANT VIII/2	ANT IX/2	ANT X/7	ANT XIII/4	ANTXV/4
Month and year	Sept. 1989	Nov. 1990	Jan. 1993	May 1996	April 98
Station_cast number	151_01	44_01	65_01	99_04	9-1; 11-2
Thickness of the WSBW[b], m	222	260	206	240	322
Potential temperature minimum along the transect, °C	-1.201	-1.143	-1.219	-1.275	-1.345
Station number	149	45	68	99	14
Pressure, dbar	1472	2908	1996	2496	3302
Salinity	34.613	34.623	34.608	34.640	34.623
Integrated potential temperature of the WSBW, °C	-0.951	-0.908	-0.953	-0.956	-1.035
Integrated area of the WSBW, km^2	43	43	37	40	56
Area of the trapezium	40	46	37	43	57
Difference between the integrated area and the trapezium, km^2	3	-3	0	-3	-1

[a] Data shown present the cruise code, the month and year of the observations, the station number of the CTD profile which was used to determine the layer thickness at mooring 207, the properties and location of the temperature minimum which was not always located at mooring 207, the mean potential temperature of the plume, the cross-section area of the plume derived from the CTD data, the cross-section area of the plume approximated by a trapezium, and the difference between the latter two areas.

[b] WSBW denotes Weddell Sea Bottom Water.

uncertainty in the depth of the -0.7°C isotherm to less than 10 m. By this means, the time series of vertical distance between the -0.7°C isotherm and the bottom was converted into a time series of cross-section area occupied by the Weddell Sea Bottom Water plume. The accuracy of this estimate is much improved compared to that obtained from simple horizontal interpolation.

4. Flow Field

The flow field within the plume was derived from the observations of the moored instruments (Figures 3 and 4 and Table 1). For this purpose the current components were rotated 17° toward the east to represent the currents parallel and

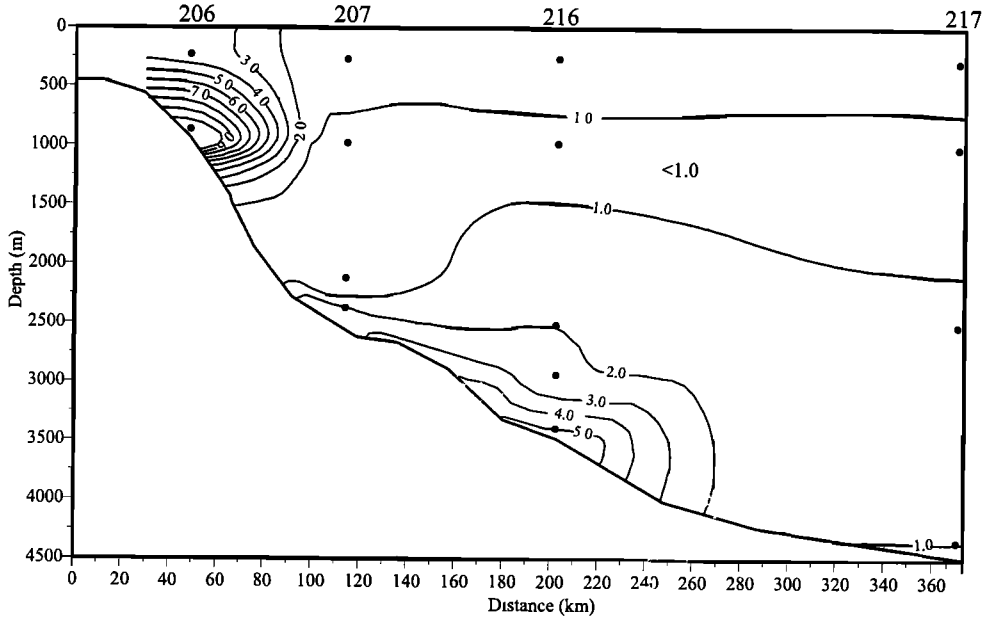

Figure 7. Vertical section along the cruise tracks as displayed in Figure 3, showing the mean current velocity parallel to the bottom contours in centimeters per second from current meters moored between January 13, 1991, and October 29, 1992. The instruments are marked by solid circles, the number of the mooring is indicated on top of the section.

Table 3. Current Meter Records Used for the Calculations in This Paper[a]

Mooring	Serial Number	Depth, m	Start Date	Duration, days	Velocity, cm	Temperature, °C
206-1	9391	876	Sept. 19, 1989	424	5.72	-1.0580
206-1	9765	229	Sept. 19, 1989	424	3.49	-0.9780
206-2	8402	260	Nov. 28, 1990	200	3.65	-1.1640
206-2	9786	900	Jan. 3, 1991	380	11.81	-0.8850
206-3	8370	280	Jan. 17, 1993	735	3.11	-1.0350
206-3	8367	930	Jan. 17, 1993	735	7.88	-0.8210
206-4	11890	246	May 14, 1996	683	1.76	-1.1650
207-1	9204	263	Sept. 20, 1989	424	1.07	0.0920
207-1	9219	952	Sept. 20, 1989	424	0.91	0.3340
207-1	9392	2162	Sept. 20, 1989	424	1.55	-0.4830
207-1	9559	2410	Sept. 20, 1989	424	3.04	-1.0500
207-2	9206	300	Nov. 29, 1990	1054	1.40	0.0960
207-2	8395	1010	Nov. 29, 1990	706	0.72	0.3580
207-2	8417	2150	Nov. 29, 1990	1309	0.25	-0.3970
207-2	8418	2410	Nov. 29, 1990	730	2.08	-1.0610
207-3	9200	344	Jan. 16, 1993	752	1.84	-0.2110
207-3	9204	1050	Jan. 16, 1993	752	1.55	0.3270
207-3	9783	2196	Jan. 16, 1993	752	3.43	-0.4320
207-3	9207	2452	Jan. 16, 1993	752	6.46	-0.9780
207-4	9207	270	May 13, 1996	686	2.36	-0.5650
207-4	1402	762	May 13, 1996	454	2.78	0.5230
207-4	9767	2187	May 13, 1996	686	3.64	-2.5060
207-4	9206	2454	May 13, 1996	1372	6.61	-1.0020
216-1	9182	2970	Nov. 30, 1990	416	2.03	-0.2770
216-1	9184	3430	Dec. 6, 1990	440	5.48	-0.8000
216-2	11926	262	May 12, 1996	688	2.21	0.4950
216-2	11885	2549	May 12, 1996	688	2.02	-0.1910
216-2	11886	3474	May 12, 1996	688	6.34	-0.8290
217-1	9192	220	Nov. 30, 1990	417	2.19	0.3000
217-1	1281	4340	Nov. 30, 1990	698	-0.40	-0.5970
217-2	10873	266	Jan. 14, 1993	740	1.94	0.5000
217-2	10540	1022	Jan. 14, 1993	740	0.35	0.1720
217-2	9782	2518	Jan. 14, 1993	740	1.27	-0.2270
217-2	9561	4374	Jan. 14, 1993	740	1.01	-0.5230

[a] The columns indicate the mooring code, the serial number of the instrument, the instruments' depth, the start date of the record, the record duration, the record mean velocity component perpendicular to the transect, and the record mean temperature.

perpendicular to the depth contours. All further calculations were done in the rotated system. Figure 7 shows the current field parallel to the depth contours averaged over the period with the best data coverage, that is, from January 1991 to October 1992. On the upper slope at 900 m depth, the annual mean currents in the bottom layer parallel to the depth contours reached a maximum speed of 11.8 cm/s. A second maximum of 5.5 cm/s occurred at 3430 m depth within the cold water plume. The velocities decreased significantly toward the Weddell Sea Deep Water layer, to less than 1 cm/s above the plume. The record length averages of measurements from the moored instruments are displayed in Table 3.

In total, the current meter records cover a time period of about 8.5 years. However, they are interrupted by three gaps of 57 to 461 days, duration during periods when the mooring array was not complete in late 1990 to early 1991, late 1992 to early 1993, and early 1995 to early 1996. During the deployment periods, data are missing at a few locations due to failure of instruments or a missing mooring (Table 1). These gaps occurred only at moorings 216 and 217, which are located at the seaward end of the bottom water plume where weak velocities are observed. Therefore they are filled with values obtained by averaging over the complete record available at that location to obtain time series of the same length for all locations. Under the condition that the currents at moorings 216 and 217 do not behave in a completely different manner during the time of the gaps than during the measurements, the method of filling the gaps does not affect the estimates of the transport variability significantly, because the transport is mainly determined by the large currents at moorings 206 and 207.

Seven of the 14 current meters were in the bottom water layer or nearby (Figure 4). The velocity data from these instruments were interpolated on a 235 km by 400 m grid parallel to the bottom line with a resolution of 1 km parallel to the bottom line and 2 m in the vertical. First, vertical profiles were obtained by linear interpolation between the two deepest instruments at each mooring (Figure 8). At mooring 207, linear extrapolation was applied from the instrument at 300 m above the bottom up to 400 m above the bottom. Then the current field between 50 km and 200 km from the shelf edge was calculated by linear interpolation parallel to the bottom line between the vertical profiles. Seaward of mooring 216 the gradient obtained at the level of the deepest

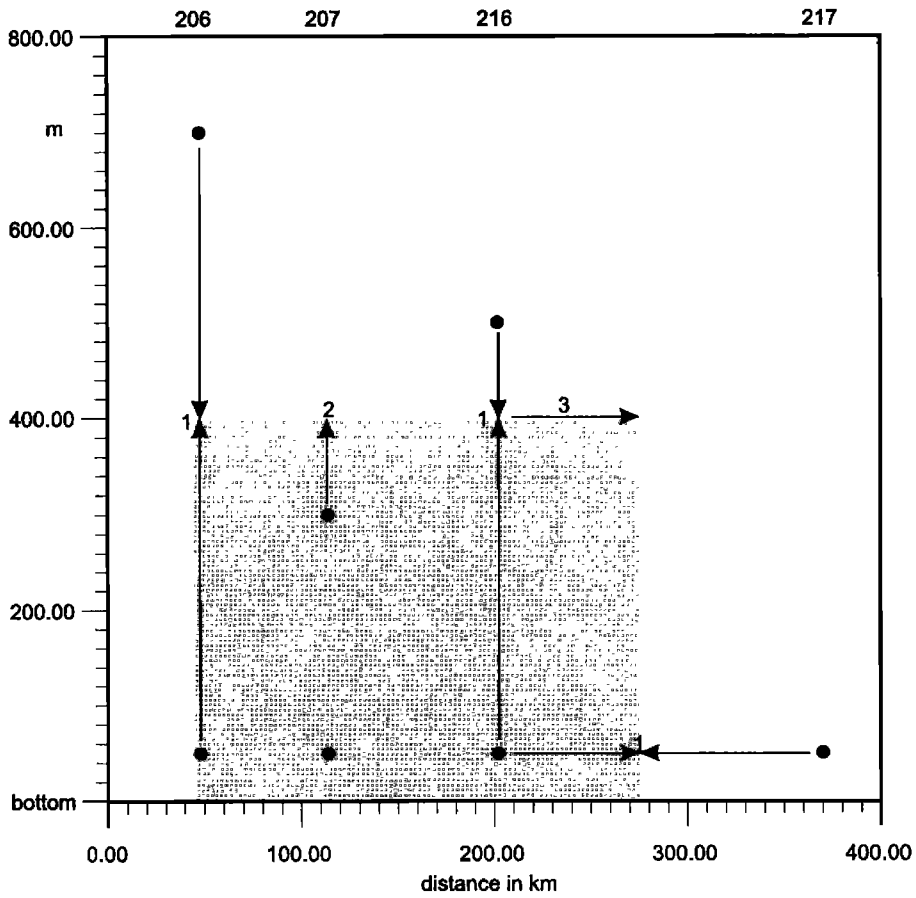

Figure 8. The locations and records used to interpolate the daily averaged current field of a 400-m-thick bottom layer from 40 to 275 km off the shelf, displayed as a shaded area. The method by which the field is obtained is indicated by numbers. Linear vertical interpolation up to the boundary is indicated by 1, linear vertical extrapolation from the current meters below by 2, and linear extrapolation along the bottom line by use of the gradient determined from the near-bottom current meters by 3.

current meters at moorings 216 and 217 was used for extrapolation parallel to the bottom line of the vertical profile obtained at mooring 216. The interpolation scheme is displayed in Figure 8. Higher-order interpolation routines were rejected to avoid nonlinear structures which cannot be justified by the available data. However, linear extrapolation over small distances within or near the bottom water plume yields more plausible fields than interpolation over much longer vertical and horizontal distances which extend into quite different oceanographic regimes.

5. Bottom Water Outflow and Its Variations

Time series of the volume transport in the bottom water plume were calculated by multiplying the plume cross-section area occupied by Weddell Sea Bottom Water and the interpolated current velocity within the plume. In a first step, time series of daily mean velocity in the plume area were estimated by averaging the daily current fields over the corresponding trapezium areas. The time series of mean plume velocity was combined with the daily values of plume cross-section area to calculate the bottom water volume transport (Figure 9). Since the distances between the instruments were greater than the baroclinic Rossby radius of deformation (between 5 km and 10 km), mesoscale structures were not resolved, and the validity of the time series is restricted to timescales longer than those of mesoscale perturbations. Therefore the time series were low-pass filtered with a 21-day running mean filter.

The outflow of bottom water fluctuates significantly on monthly, seasonal, and interannual timescales (Figure 9), ranging from -0.5 to +3.4 Sv, with an average value of 1.3±0.4 Sv, based on the low-pass filtered data. Here we will focus on the seasonal and interannual variations in bottom water transport. To obtain information about the interannual variability, the time series were split into annual periods from which the annual means were computed (Table 4).

6. Seasonal Variability

The annual cycle was determined from the 1-year-long low-pass filtered times series. First, the trend and the mean of each annual time series were removed, and then, monthly means were calculated. Finally, the monthly means of the same month from all years of which records exist were averaged (Figure 10).

The transport of bottom water is much weaker in austral summer than in winter: It reaches a minimum in December and a

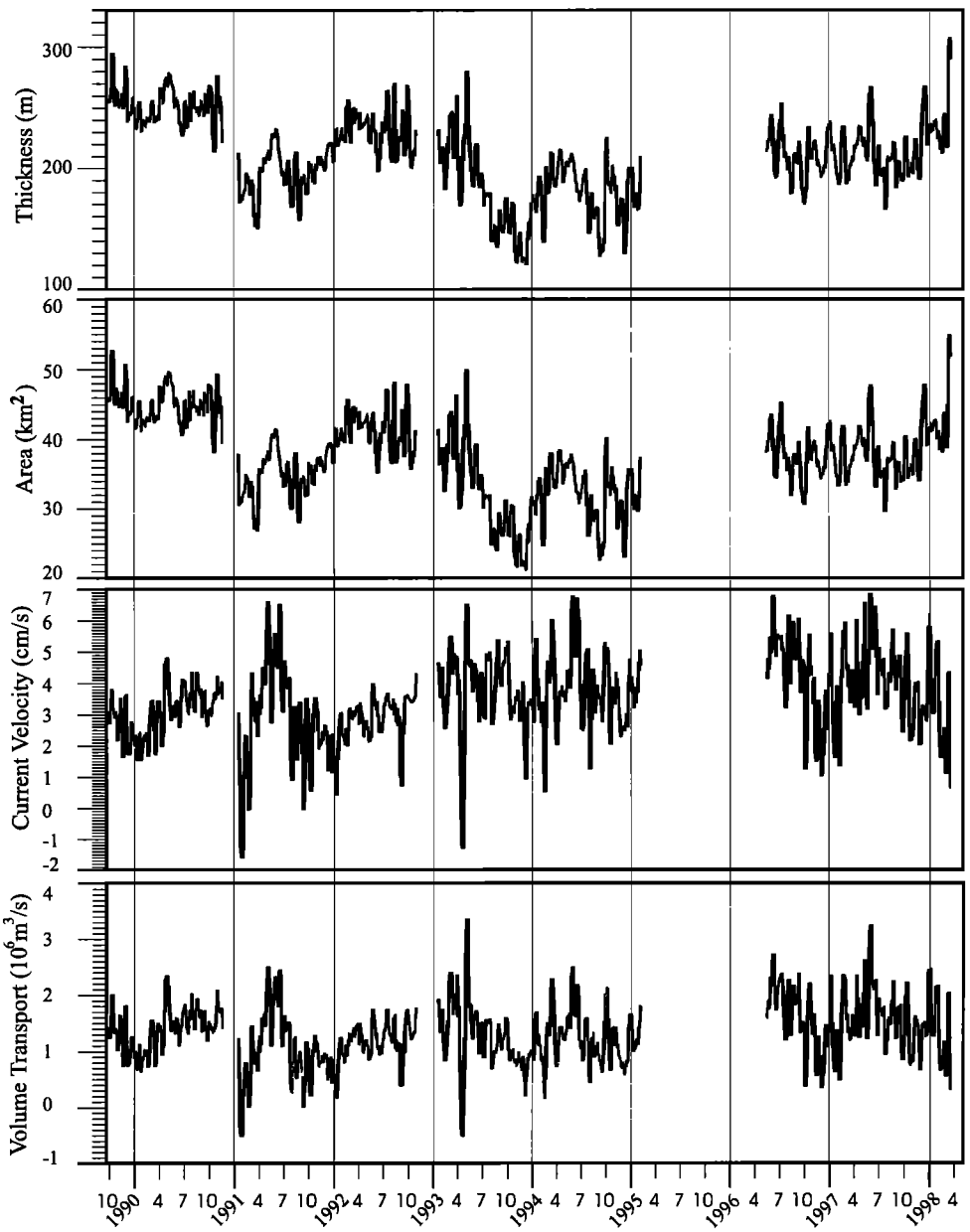

Figure 9. Smoothed time series of daily means from 1989 until 1998 of (a) the thickness of the Weddell Sea Bottom Water plume at mooring 207 as determined from the –0.7°C potential temperature, (b) the cross-section area occupied by the plume derived from the area of a trapezium which depends on the thickness, (c) the averaged cross-section current velocity for the plume, and (d) the resulting volume transport.

maximum in May (Figure 10a). The velocity is minimum in December, in phase with the transport, and maximum in June (Figure 10c). The cross-section area is minimum in August and September, about 3 months earlier than the observed minimum in transport, and maximum in May (Figure 10b). The seasonal variation of the transport around the mean is ±0.4 Sv. Taking into account the long-term mean of 1.3 Sv, the plume does not disappear during its the annual cycle, but is weakened in summer and is enhanced in early winter.

The correlations between the fluctuations in plume velocity, plume cross-section area, current velocity above the plume, and wind velocity perpendicular to the transect are used to understand the mechanisms which may force the transport variations. The transect is located north of the bottom water formation area, which can be located between the Filchner Depression and the northern boundary of the Larsen Ice Shelf. This is suggested by the observation that the bottom water plume never reached up to the shelf (Figure 5); that is, it must be fed from further south. Therefore the velocity in the plume may be controlled not only by the availability of newly formed bottom water in the source area, but also by intensity of the current system; that is, high velocities in the plume do not necessarily correlate with intensive bottom water formation, but with strong large-scale thermohaline or wind forcing. Assuming that the rates of water mass formation and outflow from the formation area remain constant, the increase in transport velocity due to wind

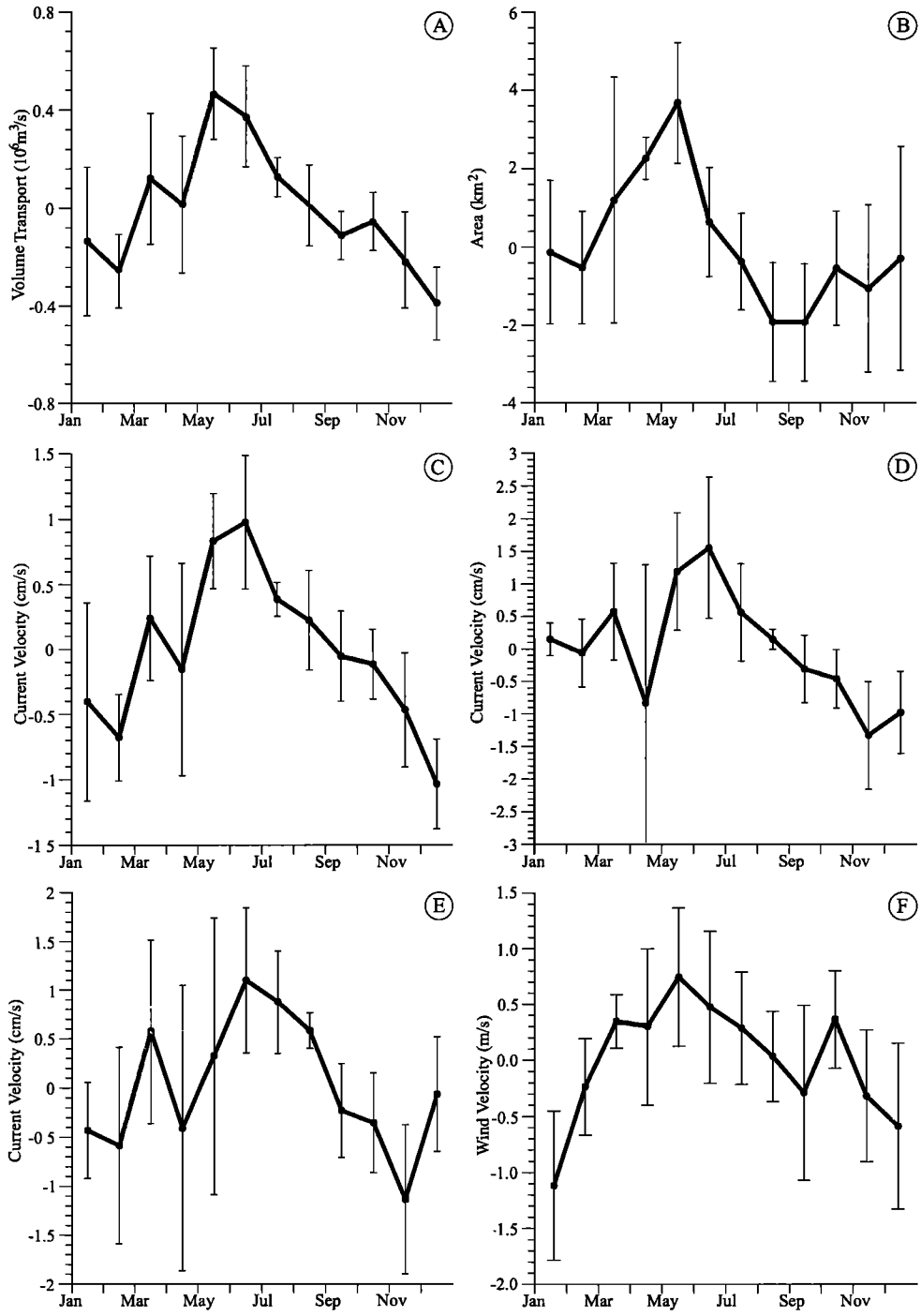

Figure 10. The mean annual cycle from 1989 until 1998 of (a) the volume transport of the Weddell Sea Bottom Water plume, (b) the area occupied by the plume, (c) the averaged cross-section current velocity for the plume, (d) the velocity at the center of the plume, 50 m above the bottom (mooring 207), (e) the velocity above the plume, 250 m below the surface (mooring 207), and (f) the wind velocity perpendicular to the transect derived from the ECMWF data set.

forcing would lead to a shrinking plume area, that is, an anticorrelation between plume velocity and cross-section area. However, an increase in bottom water formation could lead to an increase either in plume cross-section area or in plume velocity, or both.

During the annual cycle the large-scale forcing of the current system plays a significant role. The plume velocity increases in early winter simultaneously with the currents at the same position at 250 m depth (Figures 10c and 10e). Both are in phase with the wind velocity perpendicular to the transect (Figure 10f). The current velocities in the Antarctic Coastal Current in the southeastern Weddell Sea follow a similar wind-induced annual cycle with a maximum in early winter [*Fahrbach et al.*, 1992]. This suggests that the large-scale wind-induced circulation plays an important role in determining the bottom water velocities due to a barotropic velocity component which reaches a maximum in

Table 4. Estimates of Annual Means of the Characteristics and the Transport of the Weddell Sea Bottom Water Plume[a]

Year	Number of days	Thickness, m	Area, km^2	Current, cm/s	Volume Transport, $10^6 m^3/s$	Wind Component, m/s	Net Ice Export, $10^3 m^3/s$
1989	103	260	46	2.7	1.3	-	52
1990	321	250	45	3.2	1.4	0.34	46
1991	353	196	35	2.8	1.0	0.88	56
1992	303	231	41	2.8	1.2	0.22	46
1993	350	181	32	3.8	1.3	-0.13	41
1994	365	180	32	3.8	1.2	0.20	54
1995	37	179	32	4.0	1.3	0.38	49
1996	233	210	38	4.2	1.6	-0.02	33
1997	365	212	38	4.1	1.6	1.34	45
1998	87	241	43	3.1	1.3	-	-

[a] Data shown present the annual means derived from a time series from September 30, 1989, to March 18, 1998 of the thickness, the cross-section area, the mean current velocity, the volume transport of the plume, the wind velocity perpendicular to the transect, and the net sea ice export after Harms et al. (submitted manuscript, 2000). The averaging period is often less than a year.

early winter (May and June) and a minimum in summer (November and January). However, the annual cycle is more pronounced in the bottom water layer (3 cm/s) than in the shallow layers (2 cm/s), suggesting that there is a superimposed, baroclinic component leading to a strengthening of the current toward the bottom. The shear between currents 250 m below the surface and 50 m above the bottom is strongest in winter.

The bottom water is coldest and occupies the largest cross-section area in winter (Figure 11). Then, the vertical temperature difference in relation to the less variable interior ocean is largest, and a stronger horizontal gradient builds up, which in the framework of geostrophy is consistent with the intensification of the current toward the bottom. Since no salinity time series exist and the Θ/S-relationship in the plume is not constant (Table 2), we are not able to derive time series of horizontal density gradients, and consequently our arguments must remain qualitative. However, the consistent annual cycles of bottom water transport, plume velocity, plume cross-section area, velocity in the water column above the plume, and wind across the transect (Figure 10) suggest strongly that on annual timescales the bottom water outflow variability is determined not only by variations in the formation rate, but as well by the large-scale circulation in the western Weddell gyre.

7. Interannual and Longer-Term Variability

The variations on interannual timescales are of the same intensity as the annual cycle (Figure 12 and Table 4). The plume velocity increases from 2.7 cm/s in 1989 to a maximum of 4.2 cm/s in 1996 and then decreases to 3.1 cm/s in 1998. In contrast, the plume cross-section area decreases from 46 km^2 in 1989 to a minimum of 32 km^2 between 1993 and 1995 and then increases to 43 km^2. The transport varies by 14%, which is comparable in magnitude to the variability of the area (14%) and the currents (17%) (Table 5), indicating that there are interannual variations of the source strength. The bottom water transport reaches a minimum of 1.0 Sv in 1991 and a maximum of 1.6 Sv in 1996 and 1997. The variations occur on a timescale of 3 to 4 years.

If the transport fluctuations were related to variations in the water mass formation rates, we would expect the driving forces to fluctuate on similar scales. Salt release due to sea ice formation is one of the main processes affecting bottom water formation. The net export of sea ice from the southern Weddell Sea, which is directly related to the salt release, was determined by S. Harms et al. (Ice Transports in the Weddell Sea, submitted to *Journal of Geophysical Research*, 2000, hereinafter Harms et al., submitted manuscript, 2000), from measurements with

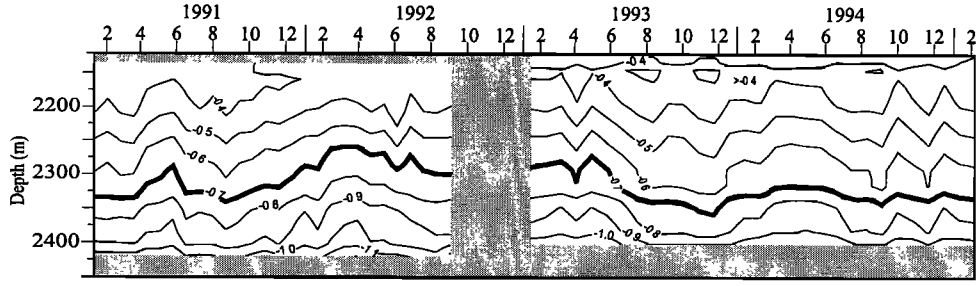

Figure 11. Isopleth diagram in °C from the temperature records of thermistor cables and adjacent current meters in mooring 207 located in the bottom water plume from 50 m to 325 m above the bottom. Since the data were referred to the water depth, the slight displacement of the mooring resulted in a shift between the two mooring periods. Months and years of measurements are given on the upper axis of the diagram.

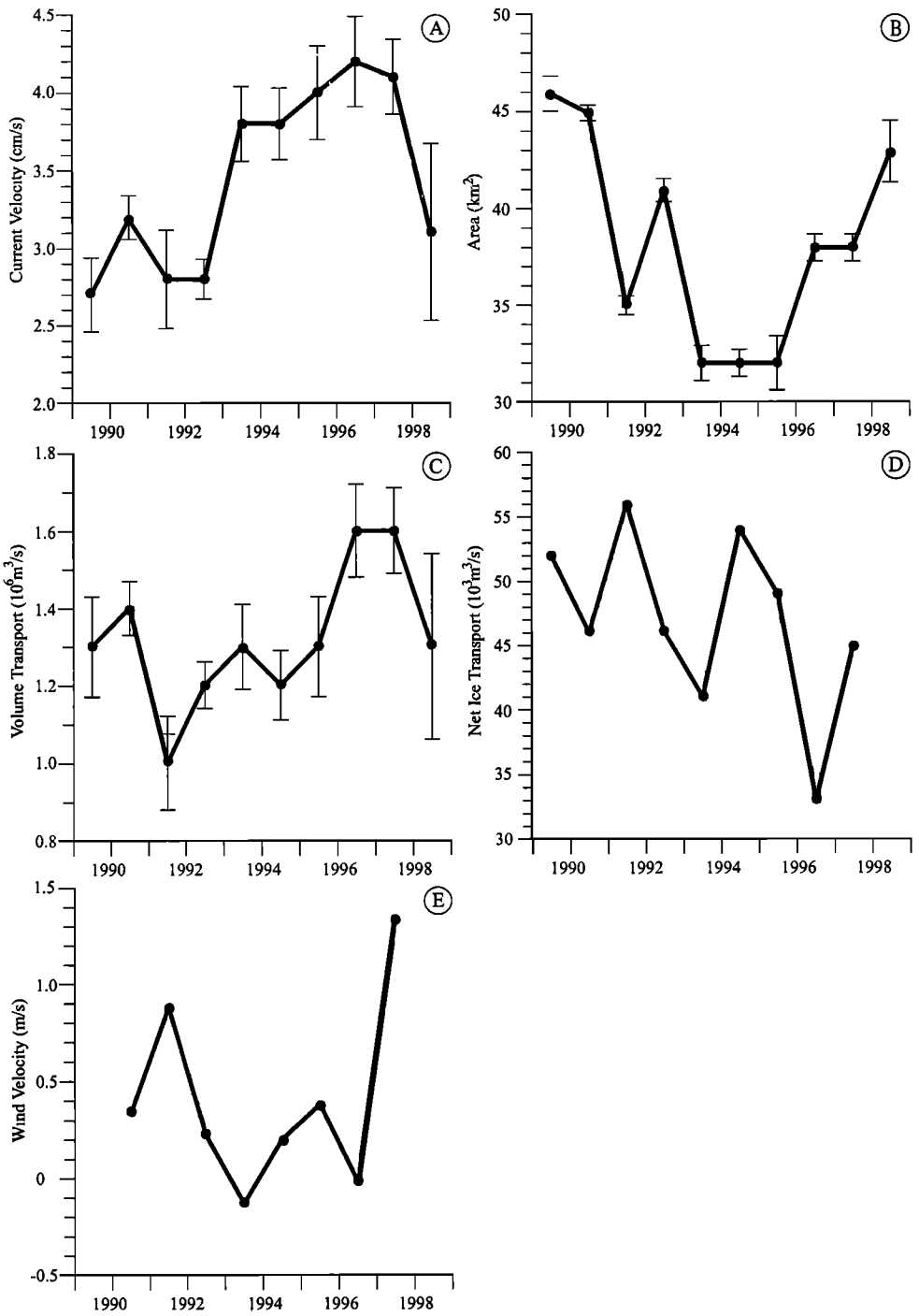

Figure 12. Time series of annual means from 1989 to 1998 of the averaged cross-section current velocity for the plume (a), the area occupied by the plume (b), the volume transport of the Weddell Sea Bottom Water plume (c), the net sea ice export as per Harms et al. (submitted manuscript, 2000) (d), and the wind velocity perpendicular to the transect derived from the ECMWF data set (e).

upward looking sonars. During the period 1989 to 1997, the annual mean ice export varied on timescales of 3 to 4 years, as did the bottom water outflow (Figures 12c and 12d). However, years with strong ice export correspond to years with low bottom water transport. This is opposite to what we expect because strong salt release should provide a large potential of bottom water production. This anticorrelation can, however, be explained by considering the delay between ice and bottom water export as well as the typical timescales of the fluctuation, that is, 3 to 4 years. First, there is a time delay between the maximum in ice export (which generates open water) and the maximum in new ice formation. Second, the newly formed bottom water takes

between a few months to some years to get from the formation areas to the transect in the northwestern Weddell Sea. If we assume a mean plume velocity of 3.5±1 cm/s and a distance to the formation area between 500 km and 1500 km, it takes between 4 months and 2 years for a pulse of newly formed water to reach the moored array. Both effects together result in the delay of 1 to 2 years between ice and bottom water export maxima. For fluctuations on timescales of 3 to 4 years, this results in an inverse phase relation.

The timescale of the observed low-frequency fluctuation of 3 to 4 years is suggestive of a relation to the Antarctic Circumpolar Wave (ACW), [*White and Peterson*, 1996]. However, the correlation is not obvious, because the ACW has a clear 4-year period, whereas in our data the period tends to be shorter. This can be understood by the interference of the externally imposed timescale of the ACW and the internal timescale of the gyre which controls the ice and bottom water transports.

Longer-term variability is indicated by the trend of the time series. The layer thickness decreased from 250 m in 1990 to 180 m in 1994 and from then on increased to 241 m in 1998 (Table 4). The trend during this period determined by a least squares fit shows a decrease of the layer thickness by 31 m over 8 years (Table 5). During the same period the plume cross-section area decreased by 5 km^2. However, because the annual mean currents increased by 1.2 cm/s between 1989 and 1998, the bottom water transport increased by 0.3 Sv. The error estimates are given in Table 5. Whereas the plume cross-section area increased by 13% of the mean and the currents by 34%, the resulting transport increased only by 23%. Since the current variability is larger than that of the transport, a significant part of the plume cross-section area variability must occur to adjust the transport to the formation rate.

8. Summary and Conclusions

In spite of significant improvement of our database, the estimate of bottom water outflow in the northwestern Weddell Sea still suffers large uncertainties. The bottom water plume area can be determined accurately (2%) only by using the data along the five CTD transects. To obtain time series, approximations have to be made which may be subject to significant errors. A comparison of the present estimate with previous calculations [Fahrbach et al., 1995] shows that although the average transports agree within the errors, variations in the transports differ, mainly due to the different analysis methods. In earlier work the plume area was estimated by shifting a fixed triangular shape vertically according to the depth change of the -0.7°C isotherm. Observations from the five sections available to date

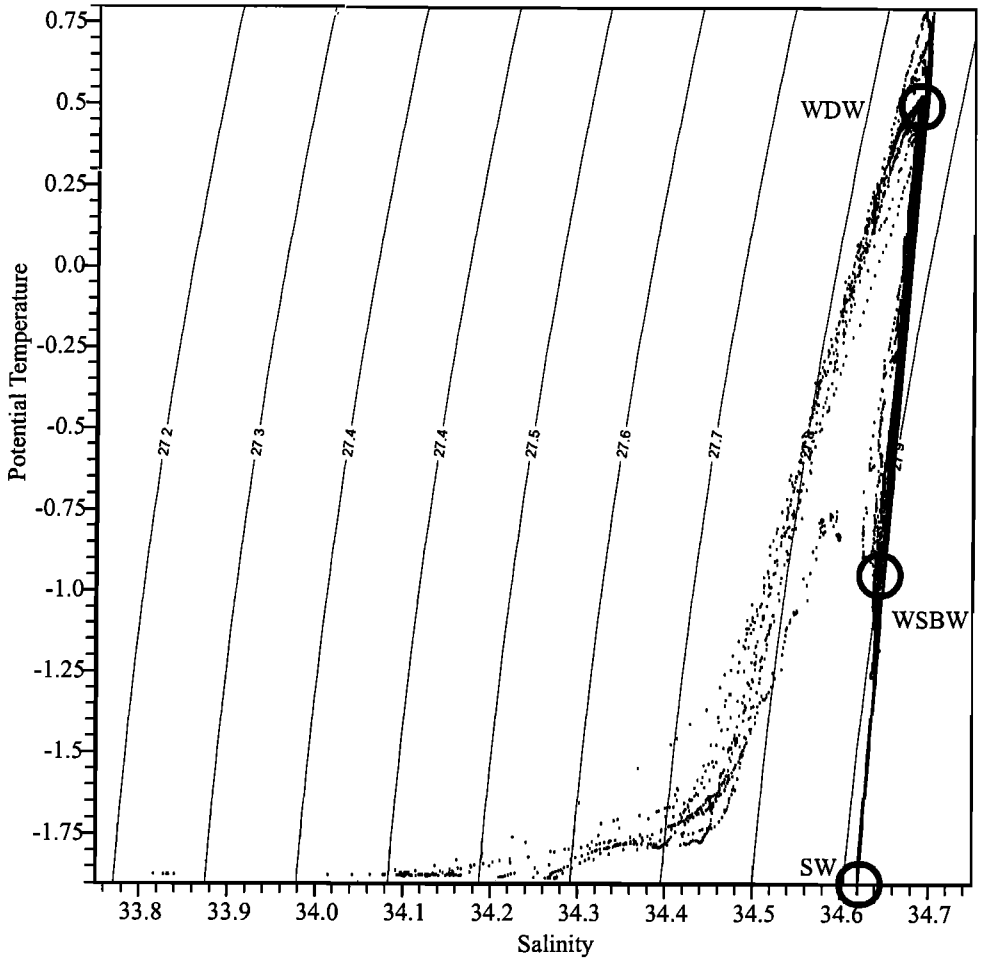

Figure 13. Potential temperature/salinity diagram from the Weddell Sea displaying the potential source water masses (Warm Deep Water = WDW and Shelf Water = SW) and the resulting Weddell Sea Bottom Water (WSBW) which is found in the plume in the northwestern Weddell Sea.

Table 5. Estimates of Long Term Means of the Characteristics and the Transport of the Weddell Sea Bottom Water Plume[a]

	Thickness, m	Area, km^2	Current, cm/s	Volume Transport, $10^6 m^3/s$	Wind Component, m/s	Net Ice Export, $10^3 m^3/s$
Mean	214	38	3.5	1.3	0.40	47
Standard deviation	30	5	0.6	0.2	0.49	7
95% Confidence of mean	21	4	0.4	0.1	0.41	5
Minimum	179	32	2.7	1.0	-0.13	33
Maximum	260	46	4.2	1.6	1.34	56
Variability	14%	14%	17%	14%	121%	15%
Trend	-31	-5	1.2	0.3	0.32	-11
Trend error	34	6	0.5	0.2	0.63	8

[a] Data shown present the average, the standard deviation, the confidence limit of the mean, the range, the relative variability of the annual means, and the trend of the time series from September 30, 1989, to March 18, 1998, of the thickness, the cross-section area, the mean current velocity, the volume transport of the plume, the wind velocity perpendicular to the transect, and the net sea ice export determined by Harms et al. (submitted manuscript, 2000). The linear trend in the records was determined by a least squares fit. The range covered by the trend from the first to the last day of the record is quoted.

suggest that it is more appropriate to approximate the plume shape by a trapezium, resulting in plume size variations which are significantly smaller than those obtained with the older method. This explains the smaller variations of the derived transports.

However, the extended database allows us to derive a longer-term average of the bottom water outflow of 1.3±0.2 Sv (based on annual means) and to eliminate to a large extent the effect of annual and interannual variability. This estimate of the contribution of the Weddell Sea to the formation of Antarctic Bottom Water does not match the generally accepted ventilation rates of the order of 10 Sv [e.g., *Orsi et al.*, 1999]. If one takes into account that the bottom water outflow does not entirely consist of newly formed water from the shelf but has incorporated a significant amount of warmer water through the entrainment of modified Warm Deep Water and Weddell Sea Deep Water, the discrepancy is even larger. By entrainment the potential temperature of the plume increases from the freezing point of -1.9°C at the sea surface to -0.95°C in the area of our observations. The Warm Deep Water, when it enters the southern Weddell Sea, has a temperature of +0.75°C, which is decreased to +0.5°C in the major formation areas (Figure 13). Therefore an entrainment rate of 60% of Warm Deep Water to 40% of fully ventilated shelf water is required to arrive at the mean temperature of -0.95°C. However, if we take further into account that a part of the entrained Weddell Sea Deep Water is not formed by mixing of Weddell Sea Bottom Water and Warm Deep Water, but enters the Weddell Sea from further to the east, the entrainment rate could be smaller. Because we can not distinguish on the basis of temperature and salinity data between the contribution of Warm Deep Water and imported Weddell Sea Deep Water of unknown ventilation rate, we can only give a range between 0.5 Sv and 1.3 Sv for the transport of recently ventilated Weddell Sea Bottom Water across our transect.

Part of the discrepancy in the estimates results from different conceptions of water mass formation or ventilation. Water mass formation can be quantified by measurements of the transport of the newly formed water mass out of the formation area, as in this paper, or by the difference between the inflow and outflow as in the works by *Fahrbach et al.* [1994] and *Yaremchuk et al.* [1998]. Ventilation consists of gas exchange with the atmosphere, which requires more time than heat and freshwater exchange. Therefore the degree of saturation of the newly formed water mass has to be taken into account. Consequently, methods based on the concentration of dissolved gases yield other formation rates than our transport measurements.

Even allowing for these discrepancies, there is a clear contradiction between our estimate and the rates required to explain ventilation rates of the deep global ocean [*Broecker et al.*, 1998, 1999]. Assuming that the latter global ventilation rates are correct, either the Weddell Sea contributes less than expected to the ventilation of the global ocean, or there are other sources supplying freshly ventilated waters in or through the Weddell Sea. In the Weddell Sea, different source areas are known [e.g., *Fahrbach et al.*, 1995; *Gordon*, 1998]. The outflow from the Filchner Depression might reach the bottom layers of the Weddell basin further south and not through the plume in the northwestern Weddell Sea. According to *Weppernig et al.* [1996], it contributes 5 Sv to the bottom water formation. Weddell Sea Deep Water formed directly from ventilated shelf water without previous Weddell Sea Bottom Water formation [*Orsi et al.*, 1993; *Fahrbach et al.*, 1995; *Orsi et al.*, 1999; *Meredith et al.*, 2000] contributes an unknown amount. Additionally, Weddell Sea Deep Water enters the Weddell Sea from the east [*Meredith et al.*, 1999, 2000] and supplies ventilated water from the Weddell Sea to the global ocean after leaving the Weddell Sea in the west. *Rintoul* [1998] identified newly ventilated water off Adélie Land and estimated that 20% of the Circumpolar Deep is ventilated from this source. A further potential source of global ventilation is located north of our observation area. Ventilation through intermediate layers could occur at the northern boundary of the Weddell Sea which is presently under investigation in the frame work of Deep Ocean Ventilation Through Antarctic Intermediate Layers (DOVETAIL). However, because of the large uncertainties in the estimates, we can not rule out the possibility that global ocean ventilation fluctuates on timescales longer than the ones covered by measurements available to date and that we are presently in a period of weak ventilation as postulated by *Broecker et al.* [1999].

Acknowledgments. We are grateful to Andreas Wisotzki, who participated in the field work, data processing, and figure production. The paper is AWI contribution 1415.

References

Baines, P. G. and S. Condie, Observations and modelling of Antarctic downslope flows: A review, *Ocean, Ice, and Atmosphere: Interactions at the Antarctic Continental Margin.* edited by S.S. Jacobs, and R. Weiss, *Antarct. Res. Ser.*, vol. 75, 29-49, AGU, Washington, D. C., 1998.

Bathmann, U., M. Schulz-Baldes, E. Fahrbach, V. Smetacek, and H.-W. Hubberten (Ed.), The expeditions ANTARKTIS IX/1-4 of the Research Vessel *Polarstern* in 1990/91, *Ber. Polarforsch., 100*, 403 pp., 1992.

Bathmann, U., V. Smetacek, H. de Baar, E. Fahrbach, and G. Krause (Ed.), The expeditions ANTARKTIS X/6-8 of the Research Vessel *Polarstern* in 1992/93, *Ber. Polarforsch.*, 135, 127 – 197, 1994.

Brennecke, W., Die ozeanographischen Arbeiten der Deutschen Antarktischen Expedition 1911-1912, *Arch. Dtsch. Seewarte, 39*, 216 pp, 1921.

Broecker, W. S., S. L. Peacock, S. Walker, R. Weiss, E. Fahrbach, M. Schröder, U. Mikolajewicz, C. Heinze, R. Key, T.-H. Peng, and S. Rubin, 1998. How much deep water is formed in the Southern Ocean? *J. Geophys. Res., 103*, 15,833-15,843, 1998.

Broecker, W. S., S. Sutherland, and T.-H. Peng, A possible 20th-century slowdown of Southern Ocean deep water formation, *Science*, 286, 1132-1135, 1999.

Carmack, E. C., Water characteristics of the Southern Ocean south of the Polar Front, in *A Voyage of Discovery*, George Deacon 70th Anniversary Vol., edited by M. Angel, pp. 15-41, Pergamon, Tarrytown, N. Y., 1977.

Carmack, E. C., Circulation and mixing in ice-covered waters, in *The Geophysics of Sea Ice*, edited by N. Untersteiner, pp. 641-712, Plenum, New York, 1986.

Carmack, E. C., and T. D. Foster, On the flow of water out of the Weddell Sea, *Deep Sea Res., 22*, 711-724, 1975.

Deacon, G. E. R., A general account of the hydrology of the South Atlantic Ocean, *"Discovery" Rep., 7*, 171-238, 1933.

European Centre for Medium-Range Weather Forecasts (ECMWF), The description of the ECMWF/WCRP Level III-A Global Atmospheric Data Archive, Reading, England, 1992.

Fahrbach, E. (Ed.), The expedition ANTARKTIS XV/4 of the Research Vessel *Polarstern* in 1998, *Ber. Polarforsch., 314*, 109 pp., 1999.

Fahrbach, E., and D. Gerdes. (Ed), The expedition ANTARKTIS XIII/4-5 of the Research Vessel *Polarstern* in 1996, *Ber. Polarforsch., 239*, 126 pp., 1997.

Fahrbach, E., G. Rohardt and G. Krause, The Antarctic Coastal Current in the southeastern Weddell Sea, *Polar Biol.*, 12, 171-182, 1992.

Fahrbach, E., G. Rohardt, M. Schröder and V. Strass, Transport and structure of the Weddell Gyre, *Ann. Geophys., 12*, 840-855, 1994.

Fahrbach, E., G. Rohardt, N. Scheele, M. Schröder, V. Strass, and A. Wisotzki, Formation and discharge of deep and bottom water in the northwestern Weddell Sea, *J. Mar. Res., 53*, 515-538, 1995.

Foster, T.D., and E.C. Carmack, Frontal zone mixing and Antarctic Bottom Water formation in the southern Weddell Sea, *Deep Sea Res., 23*, 301-317, 1976a.

Foster, T.D., and E.C. Carmack, Temperature and salinity structure in the Weddell Sea, *J. Phys. Oceanogr., 6*, 36-44, 1976b.

Gordon, A. L., Western Weddell Sea thermohaline stratification, in *Ocean, Ice, and Atmoshpere: Interactions at the Antarctic Continental Margin,* edited by S. S. Jacobs and R. F. Weiss, Antarct. *Res. Ser.*, vol. 75, pp. 215-240, AGU, Washington, D. C., 1998.

Gordon, A. L., B. A. Huber, H. H. Hellmer and A. Ffield, Deep and bottom water of the Weddell Sea's western rim, *Science, 262*, 95-97, 1993.

Mantyla, A.W., and J.L. Reid, 1983. Abyssal characteristics of the world oceans waters, *Deep Sea Res., 30*, 805-833, 1983.

Meredith, M. P., K. J. Heywood, R. D. Frew and P. F. Dennis, Formation and circulation of the water masses between the southern Indian Ocean and Antarctica: Results from $\delta^{18}O$. *J. Mar. Res., 57*, 449-470, 1999.

Meredith, M. P., R. A. Locarnini, K. A. Van Scoy, A. J. Watson, K. J. Heywood, and B. King, On the sources of Weddell Gyre Antarctic Bottom Water, *J. Geophys. Res., 105*, 1093-1104, 2000.

Mosby, H., The water of the Atlantic Ocean, *Sci. Results Norw. Antarct. Exped. 1927-1928, 1*, 1-131, 1934.

Muench, R. D., and A. L. Gordon, Circulation and transport of water along the western Weddell Sea margin. *J. Geophys. Res., 100*, 18,503-18,515, 1995.

Orsi, A.H., W.D. Nowlin Jr., and T. Whitworth III, On the circulation and stratification of the Weddell Gyre, *Deep Sea Res., 40*, 169-203, 1993.

Orsi, A. H., G. C. Johnson, and J. L. Bullister, Circulation, mixing, and production of Antarctic Bottom Water, *Prog. Oceanogr., 43*, 55-109, 1999.

Reid, J. L., and R. J. Lynn, On the influence of the Norwegian-Greenland and Weddell Seas upon the bottom waters of the Indian and Pacific Oceans, *Deep Sea Res., 18*, 1063-1088, 1971.

Reid, J.L., W. D. Nowlin Jr., and W.C. Patzert, 1977. On the characteristics and circulation of the southwestern Atlantic Ocean, *J. Phys. Oceanogr., 7*, 62-91, 1977.

Rintoul, S. R., 1998. On the origin and influence of Adélie Land Bottom Water, in *Ocean, Ice, and Atmosphere: Interactions at the Antarctic Continental Margins,* edited by S. S. Jacobs and R. F. Weiss, *Antarct. Res. Ser.,* vol. 75, pp. 151-171, AGU, Washington, D. C., 1998.

Weppernig, R., P. Schlosser, S. Khatiwala, and R. G. Fairbanks, Isotope data from Ice Station Weddell: Implications for deep water formation in the Weddell Sea. *J. Geophys. Res., 101*, 25,723-25,739, 1996.

White, W. B., and R. G. Peterson, An Antarctic circumpolar wave in surface pressure, wind, temperature and sea ice extent, *Nature, 380*, 699-702, 1996.

Wüst; G., Das Bodenwasser und die Gliederung der Atlantischen Tiefsee, *Wiss. Ergeb. Dtsch. Atl. Exped. Meteor 1925-1927, 6*(1), 1-106, 1933.

Yaremchuk, M., D. Nechaev, J. Schröter, and E. Fahrbach, A dynamical consistent analysis of circulation and transports in the southwestern Weddell Sea, *Ann. Geophys., 16*, 1024 – 1038, 1998.

E. Fahrbach, G. Rohardt, and M. Schröder, Alfred Wegener Institute for Polar- and Marine Research, Columbusstrasse, D-27568 Bremerhaven, Germany. (efahrbach@awi-bremerhaven.de)

S. Harms, Institut für Meereskunde an der Universität Kiel, Düsternbrooker Weg 20, D-24105 Kiel, Germany. (sharms@ifm.uni-kiel.de)

R. A. Woodgate, Applied Physics Laboratory, University of Washington, 1013 NE 40th Street, Seattle, WA 98105-6698. (woodgate@apl.washington.edu)

(Received May 15, 1998; revised July 28, 2000;
accepted August 23, 2000.)